

# Compact Tri-Band Microstrip Filter Using Three Types of Resonators for Bluetooth, WIMAX, and WLAN Applications

Iman Jadidi, Mohammad A. Honarvar\*, and Farzad Khajeh-Khalili

**Abstract**—In this paper, a compact tri-band microstrip filter is designed and fabricated for application in wireless communication systems such as Bluetooth, WIMAX (World Wide Interoperability for Microwave Access), and WLAN (Wireless Local Area Network). In the proposed filter, three resonators, i.e., Stub-Loaded Resonator (SLR), Stepped Impedance Resonator (SIR), and Square Split Ring Resonator (SSRR), are used. The dimensions of the proposed filter are equal to  $16.2 \times 12.3 \text{ mm}^2$  or  $0.219\lambda_g \times 0.166\lambda_g$ . These dimensions indicate that the proposed structure has reduced the size by about 40% compared to the conventional samples. This is the main advantage of the proposed filter. Finally, in order to investigate analysis and simulations, the proposed filter is fabricated. The results prove correctness of the design, analysis, and simulations.

## 1. INTRODUCTION

In recent years, for increasing needs of communications, most of wireless communication systems such as Bluetooth, WIMAX (World Wide Interoperability for Microwave Access), and WLAN (Wireless Local Area Network) have been developed and used vastly [1–3]. Microstrip filters are considered vital components and are highly required in microwave communication systems [4]. For meeting this demand, single band or wideband filters have been used [5, 6]. Also, multiband and ultra-wideband (UWB) filters substituting some single-band ones by using some technologies such as waveguides and microstrip transmission-lines are used for design [7–9]. This leads to reducing cost and dimensions of system structures. In one hand, for suitable performance and at several frequencies simultaneously, some works about the design of multiband filters by use of innovative and novel methods are presented [10–18]. These methods by use of Stepped Impedance Resonator (SIR) [10], Stub Loaded Resonator (SLR) [11], Stepped Loaded of Square Ring (SRLR) [12], and Split Ring Resonator (SRR) [13] can be suggested.

For example, a tri-band filter for covering wireless communication standards GPS (Global Positioning System), WIMAX, and WLAN by use of SIR and stepped loaded resonators are introduced [10]. The most important feature of that structure is a suitable bandwidth and simple design. However, the major disadvantage of that filter is the dependency of frequency bands to each other because of using only one type of resonator for generating all frequency bands. Also, their dimensions are relatively large. So, today for designing of microwave components, use of only SIR resonator is not suitable. So it is better to use other resonators for meeting compact dimensions. In [13], a tri-band filter for covering communication systems standards GPS, WIMAX, and WLAN with Complementary Split Ring Resonator (CSRR) structures was introduced. For enhancement of performances, CSRRs are used in the design of microwave circuits [13]. An important point in these resonators is their narrow-band frequency response. In that design, because of using CSRRs sharp skirt selectivity is achieved. According to the above references, one of the effective ways to design narrow-band performance is to use SRR and CSRR structures, and for networks that cover greater bandwidth,

---

*Received 26 January 2019, Accepted 25 March 2019, Scheduled 8 April 2019*

\* Corresponding author: Mohammad Amin Honarvar (amin.honarvar@gmail.com).

The authors are with the Department of Electrical Engineering, Najafabad Branch, Islamic Azad University, Najafabad, Iran.

is the use of SIR structures. It should be noted that SRR and CSRR structures are considered as metamaterial structures [19]. These structures are very effective in realizing high rate communication systems [19].

In this paper, a novel tri-band microstrip filter with small dimensions for covering wireless communication systems standards such as Bluetooth, WIMAX, and WLAN is proposed. For realizing this structure, three different microstrip resonators are used. The proposed filter is introduced completely in Section 2. The proposed structure consists of a stepped impedance resonator for Bluetooth (2.4 GHz), square split ring resonator for WIMAX (3.5 GHz), and stepped impedance resonator with stub-loaded, for (5.2–5.8 GHz) WLAN. Existing strong coupling among resonators and feedlines generates several Transmission Zeros (TZs) that could be improved the performance of the proposed filter.

## 2. THE PROPOSED TRI-BAND FILTER DESIGN

The proposed filter is shown in Figure 1. Its dimensions are  $12.3 \times 16.2 \text{ mm}^2$  or  $0.166\lambda_g \times 0.219\lambda_g$  where  $\lambda_g$  is the guided wavelength at 2.45 GHz. This dimension has been reduced to 40% in comparison with the sample presented in [10]. In Figure 2 the proposed resonators and other parts are presented. The optimized values of microstrip transmission-lines (TLs) and resonators gaps are reported in Table 1 (all in millimeters). The process of designing and calculating the above values will be presented.

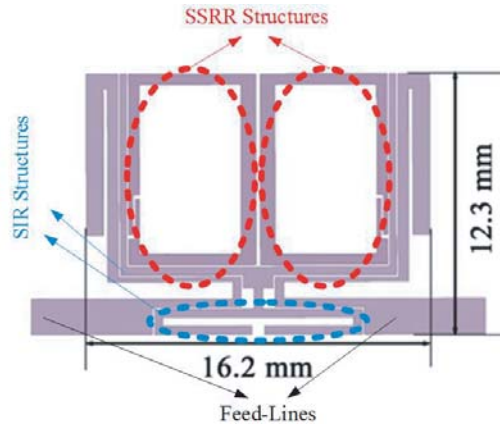


**Figure 1.** Configuration of the proposed tri-band filter.

**Table 1.** Dimensions of the proposed filter.

$L_a = 4.2$	$W_a = 0.4$	$L_b = 0.8$	$W_b = 0.4$	$L_C = 5.8$	$W_C = 0.2$
$L_d = 9.6$	$W_d = 0.7$	$L_e = 1.5$	$W_e = 0.7$	$L_f = 7.6$	$W_f = 0.8$
$L_1 = 9.1$	$W_1 = 0.3$	$L_2 = 6.5$	$W_2 = 0.4$	$L_3 = 0.6$	$W_3 = 1.4$
$L_4 = 1.0$	$W_4 = 0.4$	$L_5 = 9.9$	$W_5 = 0.4$	$L_6 = 8.0$	$W_6 = 0.7$
$L_7 = 4.8$	$W_7 = 0.5$	$L_P = 2.6$	$W_P = 0.2$	$L_S = 1.9$	$W_S = 0.2$
$g = 0.1$	$g_1 = 0.6$	$g_2 = 0.2$	$g_3 = 0.1$	$g_4 = 0.2$	$W_8 = 0.5$

### 2.1. Characteristics of the Resonators

The proposed structure consists of two parts. The first one consists of resonators 1 and 2, and the second part is resonator 3, which are shown in Figure 3. Resonator 1 is SIR; resonator 2 is Folded Stub-Loaded Stepped Impedance Resonator (FSL SIR); and resonator 3 is an SSRR.

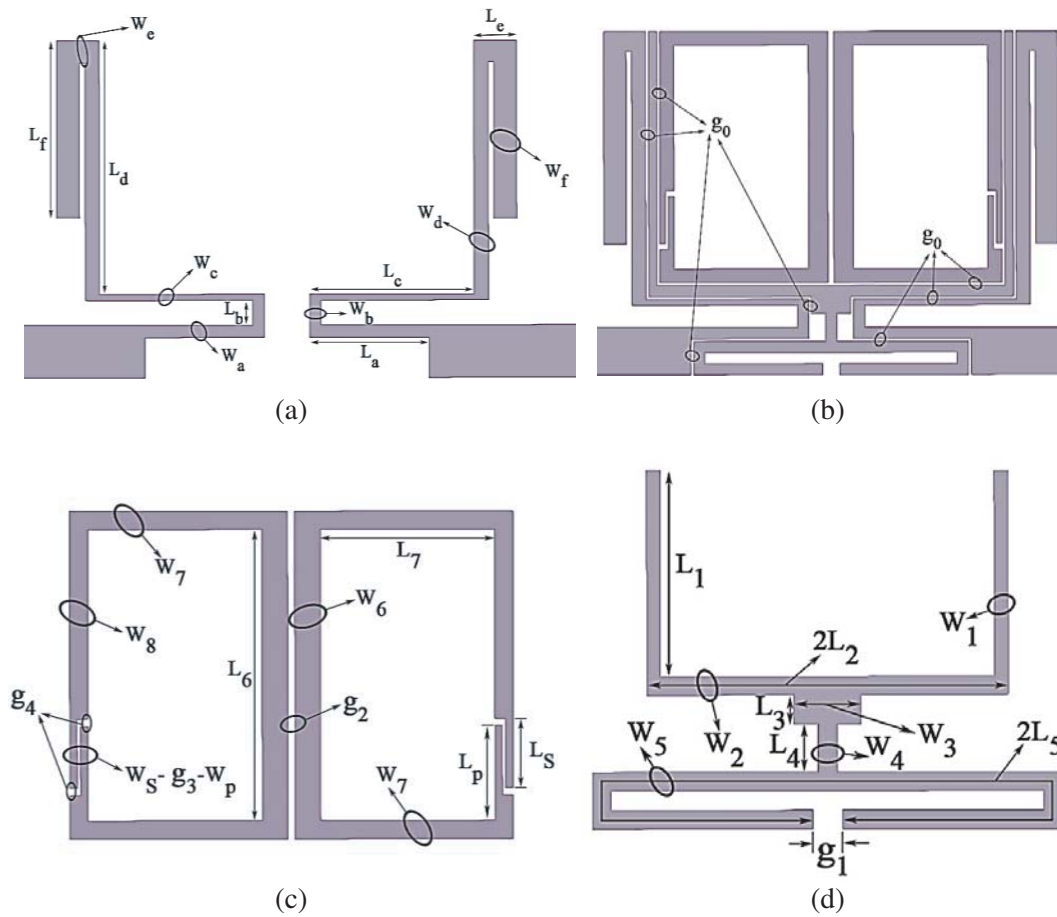


**Figure 2.** All parts of the proposed filter. (a) Final configuration, (b) configuration of feed-lines, (c) SIRs configurations, and (d) SSRR structures.

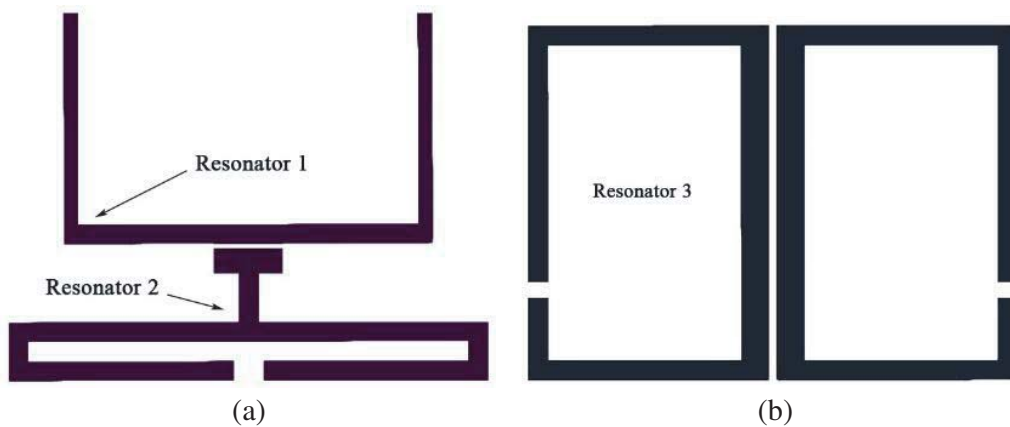


**Figure 3.** The configuration of the proposed resonators. (a) Resonators 1 and 2, and (b) resonator 3.

According to Figure 4(a), SIR and FLSIR are symmetric. So, the even and odd modes analysis can be used to determine the resonance frequencies [4]. The even and odd modes equivalent circuits of the proposed resonators are illustrated in Figure 4(b) and Figure 4(c).

According to Figure 4(b), the lines that cut the symmetry lines should be omitted, and the final

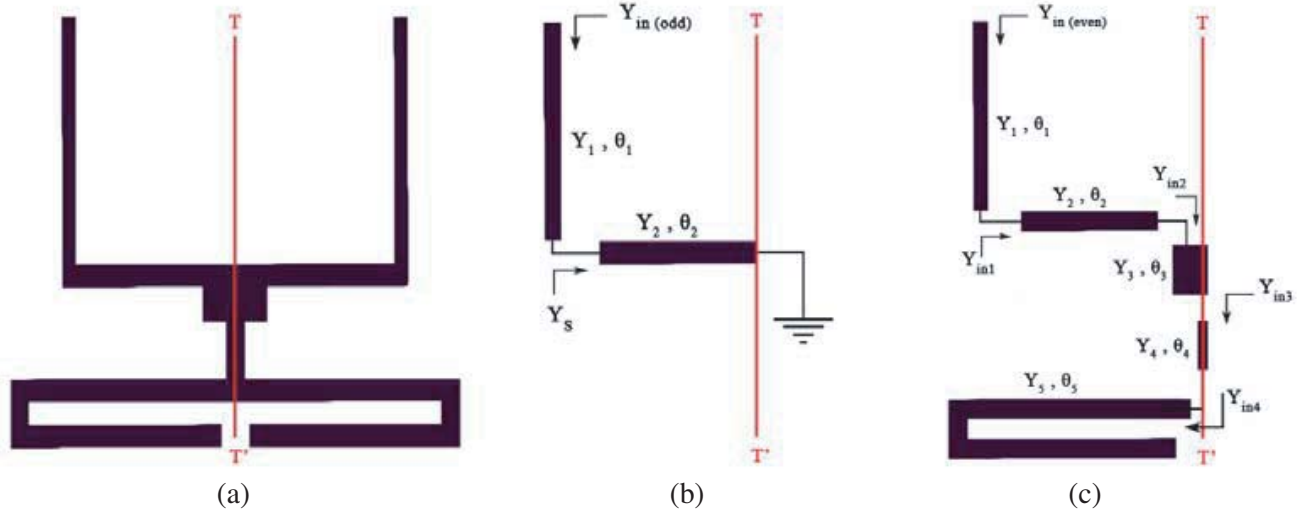


**Figure 4.** (a) The SIR and FLSIR resonators, (b) odd-mode equivalent, and (c) even-mode equivalent.

structure is connected to the ground plane [4]. So, input admittance of the odd mode circuit is:

$$Y_{in(odd)} = Y_1 \frac{(Y_s + jY_1 \tan \theta_1)}{Y_1 + jY_s \tan \theta_1} \quad (1)$$

$$Y_s = -jY_2 \cot \theta_2 \quad (2)$$

According to the relations in Eqs. (1) and (2):

$$Y_{in(odd)} = Y_1 \frac{(-jY_2 \cot \theta_2 + jY_1 \tan \theta_1)}{Y_1 + j(-jY_2 \cot \theta_2) \tan \theta_1} \quad (3)$$

Finally, with  $Y_{in(odd)}$ , the relation in Eq. (4) will be obtained:

$$\frac{Y_2}{Y_1} = \tan \theta_1 \tan \theta_2 \quad (4)$$

From the resonant condition  $Y_{in(even)} = 0$  with a little simplification and calculation, the input admittance is obtained:

$$Y_1 \left( Y_2 \frac{(A + jY_2 \tan \theta_2)}{Y_2 + jA \tan \theta_2} + jY_1 \tan \theta_1 \right) = 0 \quad (5a)$$

where  $A$  parameter is:

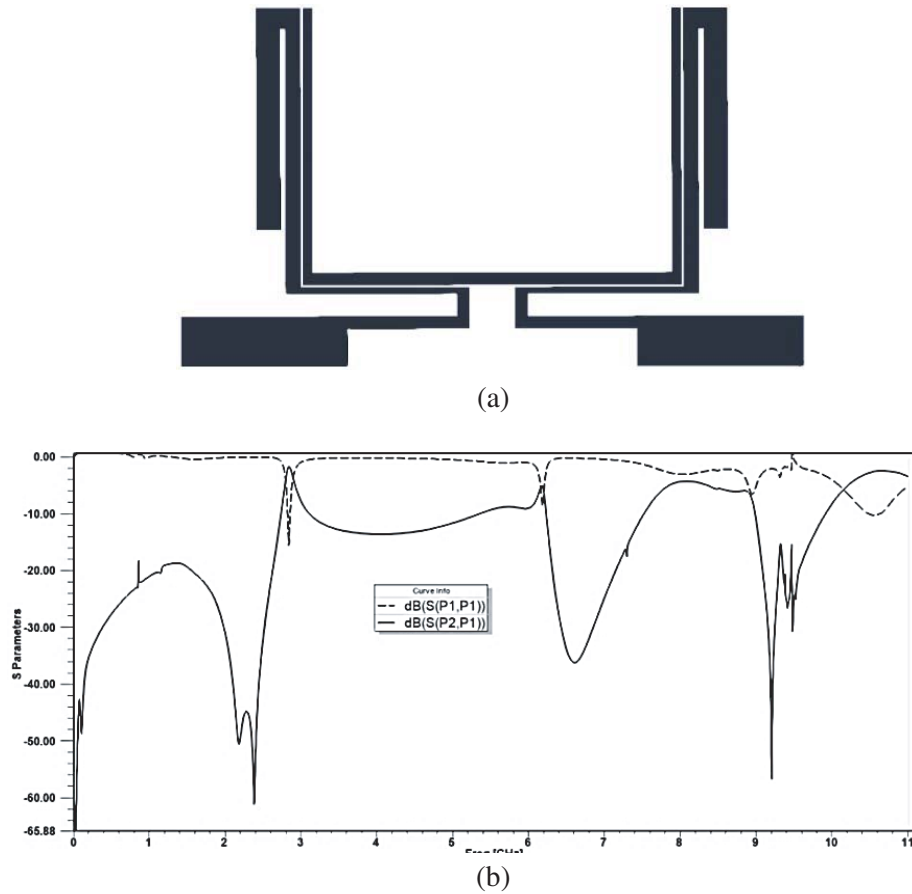
$$A = Y_3 \frac{\left( Y_4 \frac{((-jY_5 \tan \theta_5) + jY_4 \tan \theta_4)}{Y_4 + j(-jY_5 \tan \theta_5) \tan \theta_4} + jY_3 \tan \theta_3 \right)}{Y_3 + jY_4 \frac{((-jY_5 \tan \theta_5) + jY_4 \tan \theta_4)}{Y_4 + j(-jY_5 \tan \theta_5) \tan \theta_4} \tan \theta_3} \quad (5b)$$

Also, by  $Y_{in(odd)} = Y_{in(even)}$ , the positions of TZs are obtained.

## 2.2. Analysis of the Proposed Filter with Super-position Technique

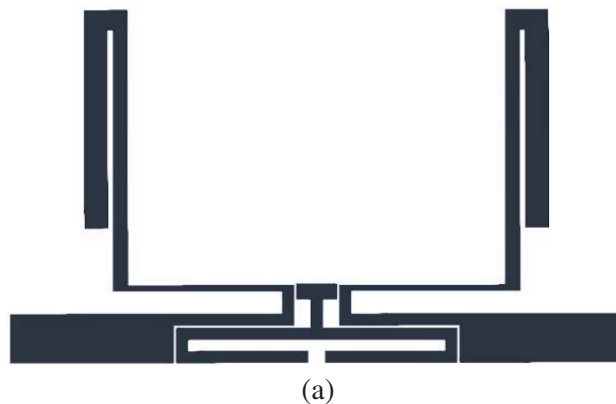
In this part, resonators are omitted, and their effects are investigated. All of the simulations are achieved by HFSSv15.0 software. The SIR and proposed feed-lines are shown in Figure 5(a). Also, the frequency responses ( $S_{11}$  and  $S_{21}$  parameters) of this structure are illustrated in Figure 5(b).

According to Figure 5(b), it is obvious that resonance frequency is around 2.8 GHz, and another is created at 6 GHz. In one hand in Figure 5(b), we can see that this resonance creates a strong TZ around 2.5 GHz and 9.2 GHz, and feedlines of structure along with FLSIR are investigated.



**Figure 5.** (a) Feed-lines and SIR structures, and (b) frequency responses of feed-lines and SIR.

In Figure 6(a) and Figure 6(b), the simulation results are presented for FLSIR structure. This structure creates a wide-resonance frequency between 5 GHz to 6 GHz frequencies, also creates a harmonic frequency around 9.5 GHz, and three TZs in 1.8 GHz, 2.4 GHz, and 6.6 GHz. From Figure 6(b) we can find that the FLSIR structure, according to the symmetry line, does not have any effect on odd-mode stimulations and just creates even-mode resonances. So, the created bandwidth by FLSIR is considered odd-mode in 5 GHz to 6 GHz. The cause of creating this frequency band is the coupling between SIR and feed-lines structures. It is clear, with the change in the locations of these parts and if adding another resonator to the proposed design, that the frequency resonances have been moved.



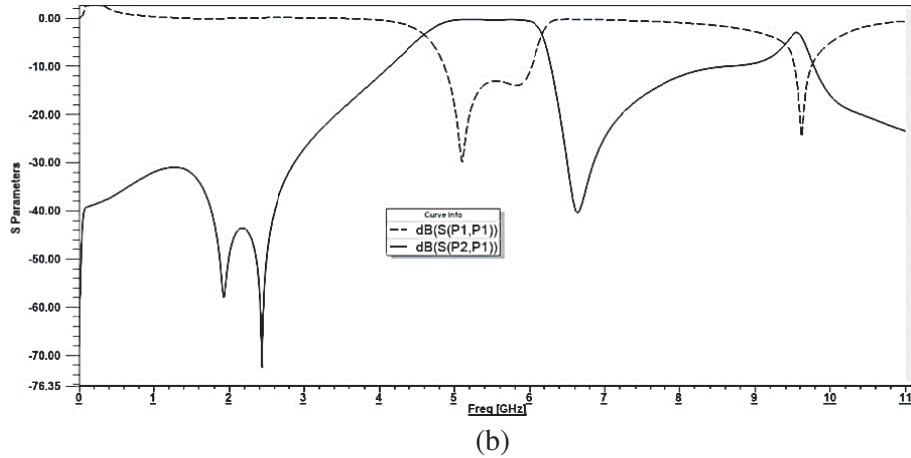


**Figure 6.** (a) Feed-lines and FLSIR structure, and (b) simulation results with feed-lines and FLSIR.

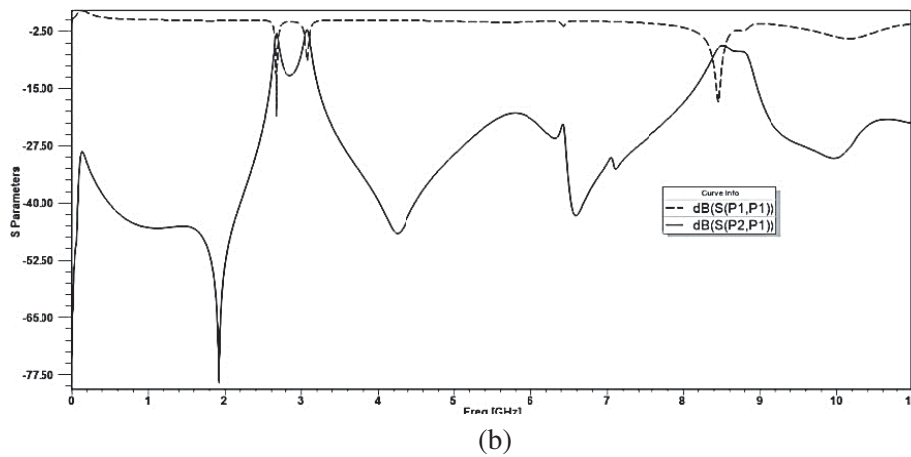
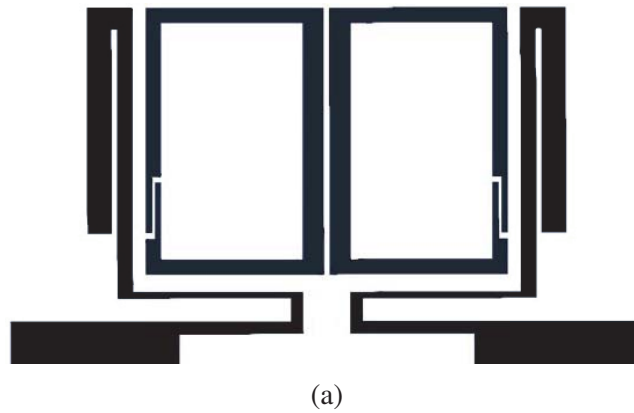


**Figure 7.** (a) Feed-lines and SSRR structure, and (b) simulation results with feed-lines and SSRR.

Thus, the purpose of presenting a super-position analysis is to determine the approximation of frequency resonances and TZs frequencies locations.

Finally, the SSRR structure with feedlines is investigated. In Figure 7(a), feedlines of structure and SSRR and, in Figure 7(b), results of simulations are shown.

According to Figure 7(b), we can see that the SSRR structures generate two resonances in 2.6 GHz

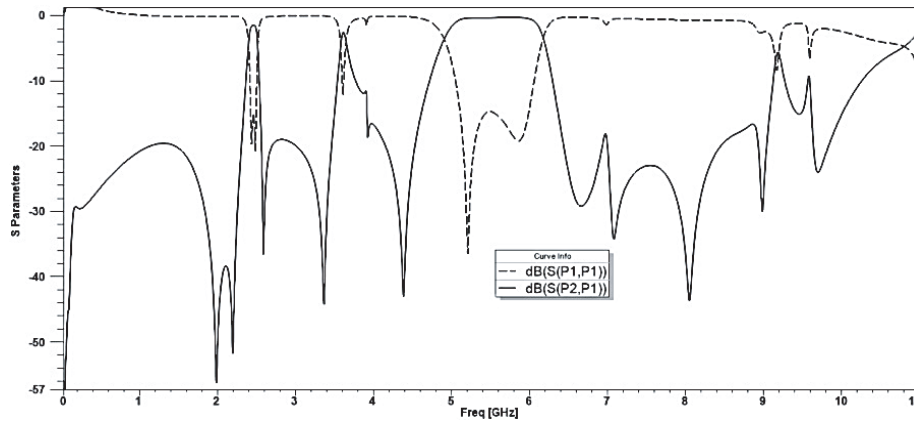


Figure 8.  $S$ -parameters of the final filter configuration.

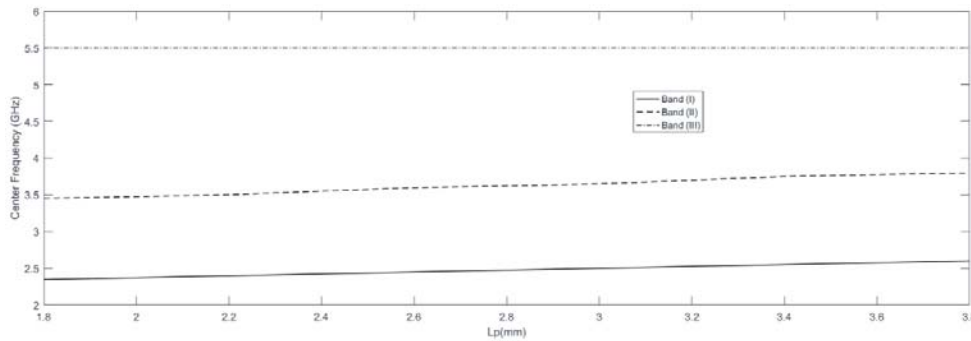


Figure 9. Effect of  $L_p$  values in resonance frequencies.

and 3.1 GHz. Also, a harmonic frequency in 8.5 GHz and a TZ in 2 GHz are created.

Finally, the total structure of filter by all existing resonators is investigated, shown in Figure 1. Simulated  $S$ -parameters of the proposed tri-band filter are illustrated in Figure 8. It can be seen that the proposed filter has the capability to cover the Bluetooth, WIMAX, and WLAN frequency bands. Note that, in the proposed structure, the electrical lengths of SSRR are increased, although the total dimension of the structure does not change. Also, the proposed technique increases the coupling between resonators and enhances insertion-loss finally [20]. In order to prove this claim, Figure 9 is shown. It can be seen that with the change in the value of  $L_p$ , the effect on the resonance frequencies represents the mentioned issue. The SSRR has a little effect on other resonators. It should be noted that changing the position of these two resonators only affects the magnitude of return-loss at the center frequencies [21].

For characterization of resonators effects, all of the transmission-losses ( $S_{21}$ ) of all the studied cases are illustrated in Figure 10.

In Figure 10, the resonators trend for creating frequency bands are characterized especially. Also, in Figure 11, the return-losses ( $S_{11}$ ) of each resonator and  $S_{11}$  results of the proposed filter are shown.

According to Figure 10 and Figure 11, the trends of resonators for creating passbands are similar. So, the third frequency band with resonator 2 (FLSIR) is created. Also, the second frequency band is created by resonator 3 (SSRR). The first frequency band is created with SIR structure. Note that the first band depends on FLSIR, although the third frequency band has a low dependency on SIR structure. As shown in Figure 11, we can say that the resonator can create TZs. Before final characterization, TZs according to Figure 12 are named.

According to Figure 12, we can see that TZ<sub>1</sub> is made because of coupling between SSRR and SIR [4]. Also TZ<sub>2</sub>, TZ<sub>6</sub>, and TZ<sub>9</sub> are introduced by coupling among feedlines and SIR. TZ<sub>3</sub> is created by coupling between FLSIR and feedlines parts. TZ<sub>5</sub> is generated by the SSRR. TZ<sub>4</sub>, TZ<sub>7</sub>, and TZ<sub>8</sub>

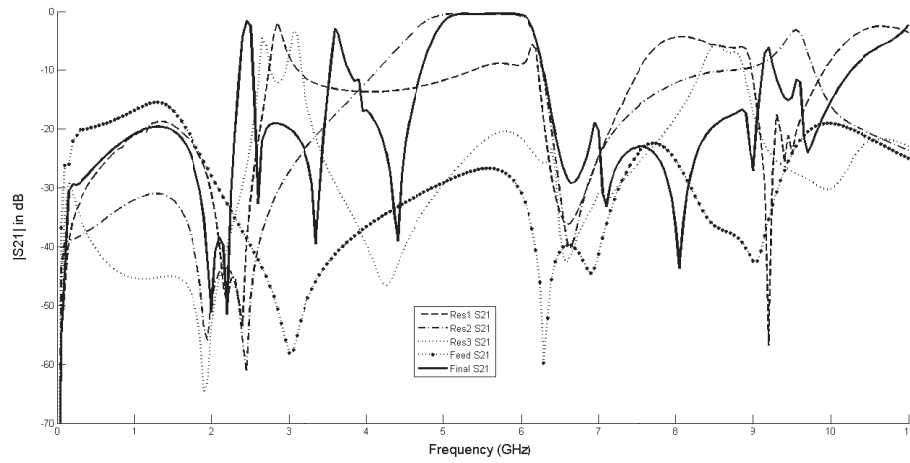


Figure 10. Insertion-losses ( $S_{21}$ ) of the proposed structure with all resonators.

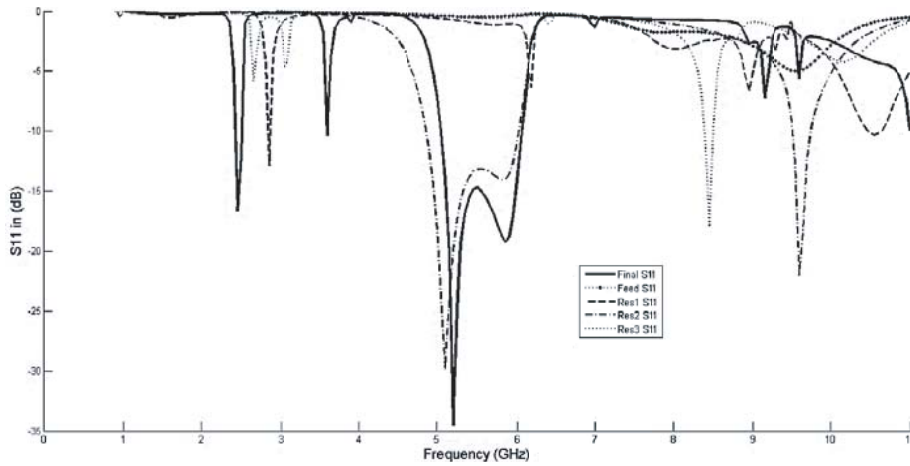


Figure 11. Return-losses ( $S_{11}$ ) of the proposed structure with all resonators.

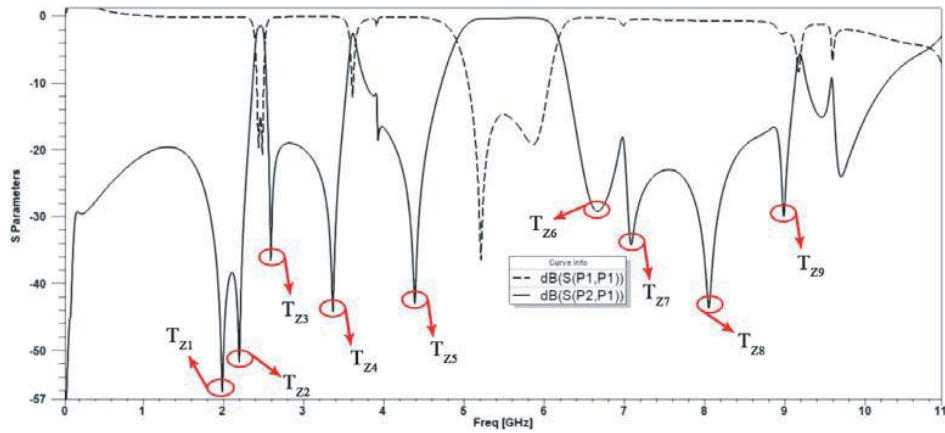


Figure 12. All TZs of the proposed filter.

are created by effects of feed-lines of the proposed filter. As clear from Figure 12, by optimizing the length and width of stubs, a harmonic frequency of SSRR resonator shifts far from the desired bands. Also, the SIR harmonic is omitted by TZ of feedlines.

### 3. FABRICATION AND MEASUREMENTS RESULTS

Now it is necessary for the realization of a tri-band filter by the capability of wireless communication networks. In Figure 13, the fabricated filter is illustrated. The simulated and measured results of  $S$ -parameters of this filter are shown in Figure 14. These results are determined by the Agilent 8722 ES Network analyzer device. As indicated in Figure 14, the results of measurements are similar to the results of simulations. A little difference is because of undesired situations of measurement devices. Passbands, insertion losses, return losses, and fractional bandwidth are reported in Table 2. Figure 15 shows a comparison of measured and simulated group delays. The maximum variation of 0.23 ns in the

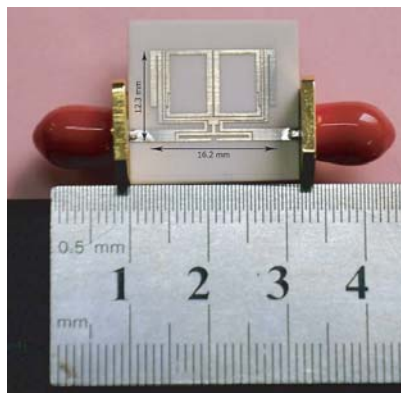


Figure 13. Photograph of the fabricated filter.

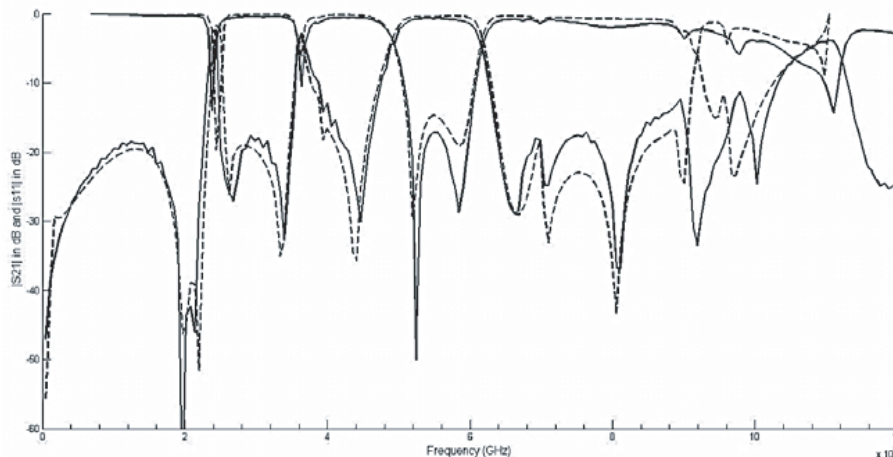
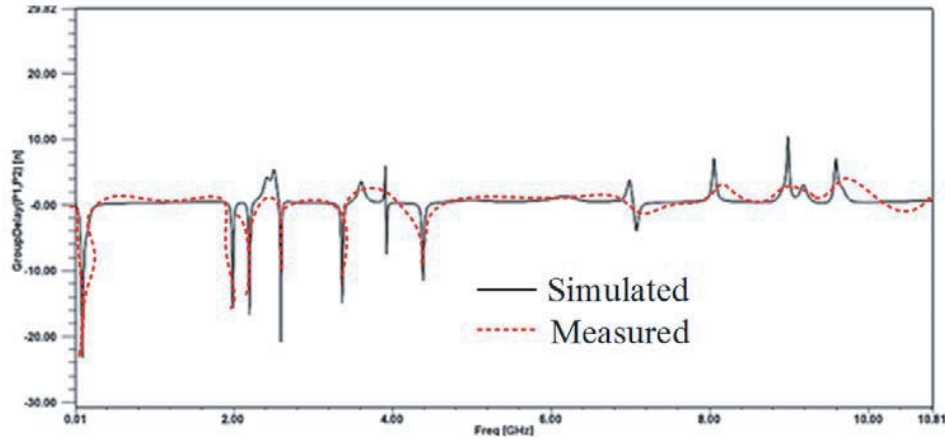


Figure 14. Simulated and measured  $S$ -parameters of the proposed filter.

Table 2. Simulated and measured results of the proposed tri-band filter.

	Passband (GHz)	Insertion Loss (dB)	Return Loss (dB)	3-dB FBW (%)	TZ
Simulation	2.45/3.6/5.5	1.5/2.4/0.4	15/13/15	4.8/1.6/25.4	9
Measured	2.44/3.6/5.5	1.6/2.2/0.5	12/14/18	4.8/2.2/25.3	10



**Figure 15.** Group delay of the proposed filter.

**Table 3.** Performance comparison of this work with other filters.

Ref.	Passband (GHz)	Insertion Loss (dB)	Return Loss (dB)	3-dB FBW (%)	TZ	Size (mm <sup>2</sup> )/(λ <sub>g</sub> × λ <sub>g</sub> )
[7]	1.95/3.5/5.2	0.46/1.96/3.9	> 16.7	8.5/3.7/3.9	3	0.38λ <sub>g</sub> × 0.28λ <sub>g</sub>
[8]	2/3.6/5.5	< 3	> 10	13.2/10.1/18.5	6	0.156λ <sub>g</sub> × 0.303λ <sub>g</sub>
[9]	2.5/5.2	< 2	> 14	6.4/5.8	4	15.6 × 8.5 mm <sup>2</sup> 0.21λ <sub>g</sub> × 0.11λ <sub>g</sub>
[11]	0.98/3.6/5.8	< 3	> 11	11/4.4/4.3	5	0.055λ <sub>g</sub> × 0.143λ <sub>g</sub>
[12]	2.4/3.5/5.5	< 1.2	> 15	11.6/6.7/17/8	4	15.6 × 8.5 mm <sup>2</sup> 0.21λ <sub>g</sub> × 0.11λ <sub>g</sub>
[13]	1.57/2.48/3.5	< 1.4	> 17.5	17.1/16.8/13.7	4	0.14λ <sub>g</sub> × 0.22λ <sub>g</sub>
[14]	1.8/2.45/3.5/5.5	< 2.3	> 15	6.7/4.2/3.7/14.8	6	19.8 × 15.8 mm <sup>2</sup> 0.19λ <sub>g</sub> × 0.15λ <sub>g</sub>
[15]	3.5/4.25/5	< 1	> 19	2/2/2	2	20 × 20 mm <sup>2</sup>
[16]	1.9/3.5/5.8	< 2	> 18	1.875/3.54/5.91	3	0.08λ <sub>g</sub> × 0.2λ <sub>g</sub>
<b>This filter</b>	<b>2.44/3.6/5.5</b>	<b>1.6/2.2/0.5</b>	<b>12/14/18</b>	<b>4.8/2.2/25.3</b>	<b>10</b>	<b>16.2 × 12.3 mm<sup>2</sup></b> <b>0.21λ<sub>g</sub> × 0.16λ<sub>g</sub></b>

passbands is noticeable. Comparisons between this work and other filters are made in Table 3. This table can well illustrate the advantages of the proposed filter.

#### 4. CONCLUSION

In this article, a compact tri-band filter is presented and analyzed. The device covers frequency bands of Bluetooth, WIMAX, and WLAN. In order to realize tri-band performance, three types of resonator structures are used. The filter has the advantage of compact size and suitable covering of standard frequency bands. Finally, in order to prove the accuracy of the carried-out simulations, the proposed structure is fabricated. The yielded results of simulation and measurement state the fact that the proposed filter has the capability to function in tri-bands for wireless communication systems.

## REFERENCES

1. Khajeh-Khalili, F. and M. A. Honarvar, "A design of triple lines Wilkinson power divider for application in wireless communication systems," *Journal of Electromagnetic Waves and Applications*, Vol. 30, No. 16, 2110–2124, Oct. 2016.
2. Kumar, R. and S. N. Singh, "Design and analysis of ridge substrate integrated waveguide bandpass filter with octagonal complementary split ring resonator for suppression of higher order harmonics," *Progress In Electromagnetics Research C*, Vol. 89, 87–99, 2019.
3. Gorur, A. K., "A novel compact microstrip balun bandpass filter design using interdigital capacitor loaded open loop resonators," *Progress In Electromagnetics Research Letters*, Vol. 76, 47–53, 2018.
4. Crnojevic-Bengin, V., *Advanced in Multi-band Microstrip Filters*, Cambridge University Press, United Kingdom, 2015.
5. Karimzadeh-Jazi, R., M. A. Honarvar, and F. Khajeh-Khalili, "High  $Q$ -factor narrow-band bandpass filter using cylindrical dielectric resonators for X-band applications," *Progress In Electromagnetics Research Letters*, Vol. 77, 65–71, 2018.
6. Shriram, S. Y., K. V. P. Kumar, and S. S. Karthikeyanc, "Compact dual-wideband bandpass filter for wireless applications," *AEU — International Journal of Electronics and Communications*, Vol. 95, 69–72, Oct. 2018.
7. Fan, W. X., Z. P. Li, and S. X. Gong, "Tri-band filter using combined E-type resonators," *Electronics Letters*, Vol. 49, No. 40, 193–194, Jan. 2013.
8. Deng, H. W., Y. J. Zhao, X. J. Zhou, Y. Fu, and Y. Y. Liu, "Design of compact and high selectivity tri-band wideband microstrip BPF," *Microwave and Optical Technology Letters*, Vol. 55, No. 2, 258–261, Feb. 2013.
9. Yan, J. M., L. Z. Cao, J. Xu, and R. S. Chen, "Design of a fourth-order dual-band bandpass filter with independently controlled external and inter-resonator coupling," *IEEE Microwave and Wireless Component Letters*, Vol. 25, No. 10, 642–644, Oct. 2015.
10. Chen, W. Y., M. H. Weng, and S. J. Chang, "A new tri-band bandpass filter based on stub-loaded step-impedance resonator," *IEEE Microwave and Wireless Component Letters*, Vol. 22, No. 4, 179–181, Apr. 2012.
11. Deng, H. W., Y. J. Zhao, Y. Fu, X. J. Zhou, and Y. Y. Liu, "Design of tri-band microstrip BPF using SLR and quarter-wavelength SIR," *Microwave and Optical Technology Letters*, Vol. 55, No. 1, 212–215, Jan. 2013.
12. Gao, L., X. Y. Zhang, and Q. Xue, "Compact tri-band bandpass filter using novel eight-mode resonator for 5G WiFi application," *IEEE Microwave and Wireless Component Letters*, Vol. 25, No. 10, 660–662, May 2015.
13. Wei, F., P. Y. Qin, Y. J. Guo, C. Ding, and X. W. Shi, "Compact balanced dual- and tri-band BPFs based on coupled complementary split-ring resonators (C-CSRR)," *IEEE Microwave and Wireless Component Letters*, Vol. 26, No. 2, 107–109, Feb. 2016.
14. Zhang, Y., L. Gao, and X. Y. Zhang, "Compact quad-band bandpass filter for DCS/WLAN/WiMAX/5G Wi-Fi application," *IEEE Microwave and Wireless Component Letters*, Vol. 25, No. 10, 645–647, Aug. 2015.
15. Sekiya, N. and S. Sugiyama, "Design of miniaturized HTS dual-band bandpass filters using stub-loaded meander line resonators and their applications to tri-band bandpass filters," *IEEE Transactions on Applied Superconductivity*, Vol. 25, No. 3, Jun. 2015.
16. Xu, J., W. Wu, and G. Wei, "Compact multi-band bandpass filters with mixed electric and magnetic coupling using multiple-mode resonator," *IEEE Transactions on Microwave Theory and Techniques*, Vol. 63, No. 12, 3909–3919, Dec. 2015.
17. Honarvar, M. A. and R. A. Sadeghzadeh, "Design of coplanar waveguide ultrawideband bandpass filter using stub-loaded resonator with notched band," *Microwave and Optical Technology Letters*, Vol. 54, No. 9, 2056–2061, Sep. 2012.
18. Mirzaei, M. and M. A. Honarvar, "Compact planar quad-band bandpass filter for application in GPS, WLAN, WiMAX and 5G WiFi," *Progress In Electromagnetics Research Letters*, Vol. 63,

- 115–121, 2016.
19. Khajeh-Khalili, F. and M. Amin Honarvar, “Novel tunable peace logo planar metamaterial unit-cell for millimeter-wave applications,” *ETRI Journal*, Vol. 40, No. 3, 389–395, Jun. 2018.
  20. Karaaslana, M., M. Bağmancia, E. Ünala, O. Akgola, and C. Sabahb, “Microwave energy harvesting based on metamaterial absorbers with multi-layered square split rings for wireless communications,” *Optics Communications*, Vol. 392, 31–38, Jun. 2017.
  21. Khajeh-Khalili, F., M. A. Honarvar, A. Dadgarpour, B. S. Virdee, and T. A. Denidni, “Compact tri-band Wilkinson power divider based on metamaterial structure for Bluetooth, WiMAX, and WLAN applications,” *Journal of Electromagnetic Waves and Applications*, Vol. 33, No. 6, 707–721, Mar. 2019.